⌘ *Author's Choice*

THE JOURNAL OF BIOLOGICAL CHEMISTRY VOL. 287, NO. 13, pp. 9855–9861, March 23, 2012

Crystal Structure of Mitochondrial Fission Complex Reveals Scaffolding Function for Mitochondrial Division 1 (Mdv1) Coiled Coil*[S]

Received for publication, November 30, 2011, and in revised form, January 26, 2012 Published, JBC Papers in Press, February 1, 2012, DOI 10.1074/jbc.M111.329359

Yan Zhang[‡1], **Nickie C. Chan**[‡§], **Huu B. Ngo**[‡], **Harry Gristick**[‡], **and David C. Chan**[‡§2]

From the [‡]*Division of Biology and* [§]*Howard Hughes Medical Institute, California Institute of Technology, Pasadena, California 91125*

Background: Mdv1 and Fis1 are components of the yeast mitochondrial fission complex.
Results: In the dimeric Mdv1-Fis1 crystal structure, the Mdv1 coiled coil mediates two protein interactions important for mitochondrial fission.
Conclusion: The Mdv1 coiled coil serves a scaffolding function in addition to dimerization.
Significance: A structural view of the dimeric Mdv1-Fis1 complex is important for understanding the mechanism of mitochondrial fission.

The mitochondrial fission machinery is best understood in the yeast *Saccharomyces cerevisiae*, where Fis1, Mdv1, and Dnm1 are essential components. Fis1 is a mitochondrial outer membrane protein that recruits the dynamin-related GTPase Dnm1 during the fission process. This recruitment occurs via Mdv1, which binds both Fis1 and Dnm1 and therefore functions as a molecular adaptor linking the two molecules. Mdv1 has a modular structure, consisting of an N-terminal extension that binds Fis1, a central coiled coil for dimerization, and a C-terminal WD40 repeat region that binds Dnm1. We have solved the crystal structure of a dimeric Mdv1-Fis1 complex that contains both the N-terminal extension and coiled-coil regions of Mdv1. Consistent with previous studies, Mdv1 binds Fis1 through a U-shaped helix-loop-helix motif, and dimerization of the Mdv1-Fis1 complex is mediated by the antiparallel coiled coil of Mdv1. However, the complex is surprisingly compact and rigid due to two additional contacts mediated by the surface of the Mdv1 coiled coil. The coiled coil packs against both Fis1 and the second helix of the Mdv1 helix-loop-helix motif. Mutational analyses showed that these contacts are important for mitochondrial fission activity. These results indicate that, in addition to dimerization, the unusually long Mdv1 coiled coil serves a scaffolding function to stabilize the Mdv1-Fis1 complex.

Mitochondrial fusion and fission are fundamental processes that control the morphology and physiology of mitochondria (1, 2). Cells with increased mitochondrial fission have fragmented mitochondria, whereas those with reduced mitochondrial fission have long and interconnected mitochondria (3–5). Mitochondrial fission is generally observed in cells undergoing apoptosis, and inhibition of mitochondrial fission can reduce or delay cell death (6). In addition, recent studies suggest that mitochondrial fission is involved in the degradation of mitochondria via autophagy (7, 8). Mitochondrial fission appears to be particularly important in neurons, and dysregulation of fission has been associated with several neurodegenerative diseases (9). Severe disruption of mitochondrial fission leads to embryonic lethality in mice (10, 11) and neonatal lethality in humans (12).

In terms of molecular mechanism, mitochondrial fission is best understood in the yeast *Saccharomyces cerevisiae*, where the core machinery has been identified through genetic screens (3, 13–15). Mitochondrial fission requires recruitment of the dynamin-related GTPase Dnm1 (3–5) onto the surface of mitochondria, where it mediates constriction and fission. Genetic and biochemical studies indicate that recruitment of Dnm1 requires the mitochondrial outer membrane protein Fis1. Fis1 recruits Dnm1 via one of two molecular adaptors, Mdv1 or Caf4 (16–18). Yeast with null alleles of Fis1, Dnm1, or Mdv1 show severe defects in mitochondrial fission, resulting in interconnected net-like mitochondria (3, 13–15). Removal of Caf4 does not result in an obvious mitochondrial morphology defect unless Mdv1 is also absent (17). In mammalian cells, there are orthologs for Dnm1 and Fis1 but not for Mdv1 or Caf4. Several studies support a role for Fis1 in mammalian mitochondrial fission (19–22), but a recent study indicates that another outer membrane protein, Mff (23), may be the primary receptor for Drp1 (24). Therefore, the fission machinery in mammals is currently much less understood than that in yeast.

To elucidate the molecular mechanism, it is critical to gain a structural understanding of the mitochondrial fission complex. By binding both Fis1 and Dnm1, Mdv1 plays a pivotal role in coordinating the mitochondrial fission complex. Domain analysis indicates a simple modular structure that is well suited for

* This work was supported, in whole or in part, by National Institutes of Health Grants GM083121 and GM062967.
⌘ *Author's Choice*—Final version full access.
[S] This article contains supplemental Figs. S1 and S2.
The atomic coordinates and structure factors (code 3UUX) have been deposited in the Protein Data Bank, Research Collaboratory for Structural Bioinformatics, Rutgers University, New Brunswick, NJ (http://www.rcsb.org/).
[1] Supported in part by a postdoctoral fellowship from the American Heart Association.
[2] To whom correspondence should be addressed: Howard Hughes Medical Institute, California Institute of Technology, 1200 E. California Blvd., MC114-96, Pasadena, CA 91125. Tel.: 626-395-2670; Fax: 626-395-8826; E-mail: dchan@caltech.edu.

its adaptor function. Mdv1 (as well as Caf4) contains three domains with distinct activities important for mitochondrial fission. The N-terminal extension (NTE)[3] region binds to Fis1; the coiled-coil region mediates Mdv1 dimerization; and the C-terminal WD40 repeat region binds to Dnm1 (16–18). Structural studies have clarified how Mdv1 and Caf4 use the NTE region to bind Fis1 (25) and how the Mdv1 coiled-coil region mediates dimerization (26). Here, we have extended these studies by solving the crystal structure of a larger dimeric Mdv1-Fis1 complex. Surprisingly, we found that the Mdv1 coiled coil serves not only as a dimerization interface but also as a scaffold for additional protein interactions that are important for mitochondrial fission.

EXPERIMENTAL PROCEDURES

Expression and Purification of Mdv1-Fis1 Complex—The Mdv1-Fis1 complex was purified from Rosetta(DE3) bacterial cells coexpressing Fis1 and Mdv1. Yeast Fis1(1–129), lacking the transmembrane segment, was amplified by PCR and cloned into the pBB75 vector. Mdv1(94–314), containing the NTE and coiled coil, was cloned into the pET15b vector, which encodes an N-terminal His_6 tag. Mutations K215A and K216A were introduced into the Mdv1 construct by PCR with oligonucleotides encoding the mutations. Rosetta(DE3) cells harboring both the Fis1 and Mdv1 constructs were cultured at 37 °C until A_{600} = 0.6–0.8. The temperature was then lowered to 22 °C, and isopropyl β-D-thiogalactopyranoside was added to a final concentration of 0.3 mM to induce protein expression. After 8 h of induction, the cells were harvested by centrifugation. All purification steps were carried out at 4 °C. The cell pellets were resuspended in lysis buffer (50 mM sodium phosphate and 300 mM sodium chloride (pH 7.4)) and disrupted by sonication. The clarified cell lysate was applied to TALON resin (Clontech) pre-equilibrated in lysis buffer. The resin was extensively washed with lysis buffer containing 10 mM imidazole. The protein complex was eluted from the resin with lysis buffer containing 100 mM imidazole. The Mdv1-Fis1 complex was further purified on a HiLoad 16/60 Superdex 200 column (GE Healthcare) by gel filtration chromatography. The purified complex was dialyzed against 20 mM Tris (pH 8.0) and concentrated to 11 mg/ml.

Crystallization and Structure Determination—The Mdv1-Fis1 complex was crystallized at 22 °C using the hanging-drop vapor-diffusion method. Each drop, containing 2 μl of protein complex and 2 μl of reservoir solution, was equilibrated against 400 μl of reservoir solution. The reservoir solution for the optimized condition contained 0.54 M sodium citrate, 0.1 M cacodylate (pH 6.8), and 4% acetonitrile. The crystals were cryoprotected by dipping stepwise into mother liquor containing 15% glycerol and then 25% glycerol. The crystals were flash-frozen in liquid nitrogen.

X-ray diffraction data sets from two crystals were collected at the Stanford Synchrotron Radiation Lightsource at beamline 9-1 with a Quantum-315 CCD detector (Area Detector Systems Corp.). The crystals belong to space group I422 with unit cell parameters a = 174.7, b = 174.7, and c = 167.3 Å. The crystals have a solvent content of 72%, with two Mdv1-Fis1 complexes per asymmetric unit. Both data sets were integrated with the XDS package (27) and then combined with Pointless (28) in the CCP4 suite. The integrated reflections were scaled using Scala (28). The phases were determined by molecular replacement in Phaser (29) using the previously solved, smaller Mdv1-Fis1 complex (Protein Data Bank code 2PQN) (25) and one chain of the coiled-coil structure (code 2XU6) (26) mutated to polyserine as the search models. Refinement was performed using REFMAC (30) and CNS with Ramachandran restraints, followed by manual remodeling with the molecular graphic program Coot (31). In the final model, 94.8% of side chains were in preferred regions, 4.0% in allowed regions, and 1.2% in disallowed regions.

Circular Dichroism—Circular dichroism data were collected on an Aviv 62DS spectrometer with a 1-mm path length cell. Spectra were collected in 50 mM Na_2HPO_4 (pH 7.4) and 300 mM NaCl at 25 °C. Recombinant Mdv1-Fis1 complexes were analyzed at a concentration of 8 mM.

Co-immunoprecipitation Assay—A yeast strain (JSY9541) (26) lacking Fis1, Mdv1, and Caf4 (*MAT***a** *leu2Δ1 his3Δ200 trp1Δ63 ura3-52 lys2Δ202 mdv1*::*HIS3 caf4*::*KanMX fis1*::*HIS3*, a gift from Janet Shaw) was used for all the functional studies. Mitochondrially targeted DsRed was integrated into the cells to monitor mitochondrial morphology. For co-immunoprecipitation experiments, Myc-Fis1 and HA-Mdv1 were expressed from the *MET25* (methionine-repressible) promoter. Yeast cells were cultured in synthetic dextrose medium containing 0.1 mg/ml methionine. Immunoprecipitations were performed as described previously (25, 26). Briefly, 40 A_{600} units of cells were lysed with glass beads. The clarified cell lysate was applied to 40 μl of agarose beads conjugated with anti-c-Myc antibody (Sigma-Aldrich) and incubated at 4 °C for 90 min. Protein samples were analyzed by SDS-PAGE and Western blotting with anti-Myc antibody 9E10 or anti-HA antibody 12CA5.

Mitochondrial Localization and Morphology Analysis—Fluorescence microscopy was used to determine the subcellular localization of GFP-Mdv1. Fis1 variants and GFP-Mdv1 variants were expressed from the *MET25* promoter in the *fis1Δmdv1Δcaf4Δ* yeast strain containing Mito-DsRed. Cells were cultured to mid-log phase in synthetic dextrose medium containing 0.1 mg/ml methionine and then diluted into medium without methionine. Cells were grown for another 2 h before scoring GFP-Mdv1 localization *versus* Mito-DsRed.

Mitochondrial morphology was scored in the yeast strains used for immunoprecipitation. Cells were grown in medium containing 0.1 mg/ml methionine to mid-log phase. Mitochondrial morphology was scored using a 100× oil immersion objective (Nikon Instruments Inc.). For each strain, >300 cells from three independent clones were scored with a 100× oil immersion objective.

RESULTS

Overview of Dimeric Mdv1-Fis1 Structure—Our previous crystal structure of Mdv-Fis1 was monomeric because the Mdv1 fragment lacked the coiled-coil region that is important for dimerization (25). To gain a structural understanding of the dimeric Mdv1-Fis1 complex, we attempted to crystallize a complex of the cytosolic domain of Fis1 (residues 1–129) bound to a larger Mdv1 fragment (residues 93–314) that contains both the

[3] The abbreviation used is: NTE, N-terminal extension.

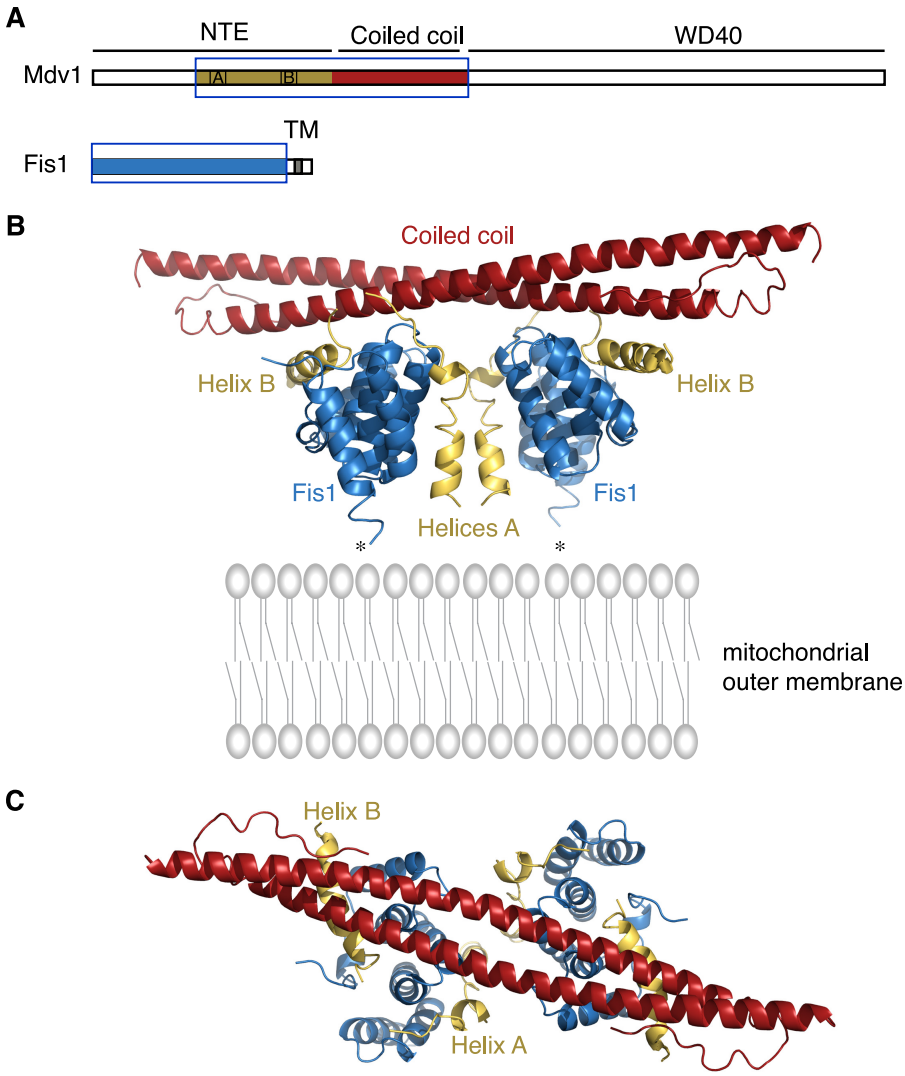

FIGURE 1. **Structure of Mdv1-Fis1 complex.** *A*, schematic diagram showing the domains in Mdv1 and Fis1. In Mdv1, the NTE region, the coiled coil, and the WD40 repeat region are indicated. Within the NTE region, the locations of helices αA and αB are highlighted. In Fis1, the transmembrane (*TM*) segment is indicated. The regions contained in the crystallized Mdv1-Fis1 complex are indicated by *blue boxes* and color-coded as in *B* and *C*. *B*, side view of the Mdv1-Fis1 dimer. For orientation, the expected plane of the mitochondrial outer membrane is shown. The Fis1 molecules are depicted in *blue*. The C-terminal ends of the Fis1 molecules are indicated by *asterisks*; the transmembrane helices would be expected to extend from these ends and insert into the outer membrane. The Mdv1 helix-loop-helix motif is shown in *yellow*, and the Mdv1 coiled coil is shown in *red*. *C*, top view of the Mdv1-Fis1 complex showing that the Mdv1 coiled coil lies on top of the Fis1 molecules.

NTE region and the coiled coil. However, the crystals diffracted only to 7 Å. To engineer a variant with better crystal lattice-forming propensity, we applied surface entropy reduction analysis (32) and identified two lysine residues that were predicted to disfavor crystallization. These two lysine residues (Lys-215 and Lys-216), located between the NTE and coiled-coil domains, were substituted with alanine (Fig. 1*A*). The resulting Mdv1-Fis1 complex was crystallized and indeed diffracted to a better resolution of 3.9 Å. The crystals belong to space group I422, with two Mdv1-Fis1 complexes per asymmetric unit (Table 1).

The Mdv1-Fis1 complex forms a surprisingly compact dimer with 2-fold symmetry. In the side view depicted in Fig. 1*B*, the plane of the mitochondrial outer membrane would be located at the bottom. The cytosolic region of Fis1 lies above the mitochondrial outer membrane. Each Fis1 molecule in the dimer is bound by a U-shaped helix-loop-helix motif of Mdv1, as detailed below. Above the Fis1 molecules lies the dimeric antiparallel coiled coil of Mdv1 (Fig. 1, *B* and *C*). This coiled coil has a length of 106 Å and provides an unusually long interface for dimerization. Our coiled-coil structure agrees well with the previous crystal structure of the isolated coiled coil (root mean square deviation of 1.36 Å for backbone atoms) (Fig. 2*A*) (26). The latter structure was slightly truncated by a few residues compared with our structure.

Helix-Loop-Helix Motif in Mdv1 Wraps around Fis1 Surface—Fis1 organizes into a six-helix bundle (helices α1–α6) (Fig. 2*B*) (25, 33–36). Within these six helices, the helical pairs α2/α3 and α4/α5 constitute tetratricopeptide-like motifs that have a helix-turn-helix structure. The Fis1 helical bundle has a convex and a concave surface. In our previous structural analysis of the Caf4-Fis1 complex, we found that Caf4 utilized a U-shaped helix-loop-helix (αA-loop-αB) motif in the NTE domain to bind both surfaces of Fis1 (25). The αA helix of Caf4 bound to the convex side of Fis1, whereas the C-terminal αB helix bound to the concave side. We also obtained the structure of a shorter Mdv1-Fis1 complex in which helix αB, but not helix αA, of Mdv1 was present. On the basis of the sequence similarity

TABLE 1
Data collection and refinement statistics (molecular replacement)

	Mdv1-Fis1
Data collection	
Space group	I422
Cell dimensions	
a, *b*, *c* (Å)	174.7, 174.7, 167.3
α, β, γ	90.0°, 90.0°, 90.0°
Resolution (Å)	20-3.9
R_{sym} or R_{merge}	0.076 (0.519)[a,b]
$I/\sigma I$	25.0 (4.6)[a]
Completeness (%)	98.9 (98.1)[a]
Redundancy	14.5 (8.1)[a]
Refinement	
Resolution (Å)	20-3.9
No. reflections	11999
R_{work}/R_{free}	0.269/0.284
No. atoms	
Protein	4078
B-factors	
Protein	126.7
r.m.s.d.[c]	
Bond lengths (Å)	0.021
Bond angles	1.94°

[a] Values in parentheses are for highest resolution shell.
[b] Two data sets were collected on two different crystals. The data sets were combined and scaled together (see "Experimental Procedures" for details).
[c] r.m.s.d., root mean square deviation.

of Mdv1 to Caf4, we predicted that Mdv1 would contact Fis1 via a similar U-shaped αA-loop-αB motif, even though we lacked direct structural evidence for this idea (25). Two-hybrid and biochemical studies showed that both interfaces were essential for binding of Mdv1 to Fis1. Moreover, mutations in the predicted αB helix of Mdv1 abrogated mitochondrial fission activity (25).

Our crystal structure clarifies the mechanism of Mdv1 binding to Fis1 by providing direct evidence that Mdv1 uses the αA-loop-αB motif to wrap around the helical bundle of Fis1 (Fig. 2, *B* and *C*). These interactions are largely through hydrophobic contacts. This portion of the Mdv1-Fis1 structure superimposes well with the previous Caf4-Fis1 structure (root mean square deviations of 0.81 Å for Fis1 and 1.66 Å for helices αA and αB) (Fig. 2*B*). The mutations in this motif that were shown to impair Fis1 binding to Mdv1 and mitochondrial fission (25) are mapped onto this structure in Fig. 2 (*D* and *E*). In particular, it can be seen that contacts between the Mdv1 αA helix (missing in our previous structure) and the convex surface of Fis1 are essential for mitochondrial fission.

Two Contact Sites on Surface of Mdv1 Coiled Coil—Although the αA-loop-αB motif in Mdv1 clearly provides the major binding

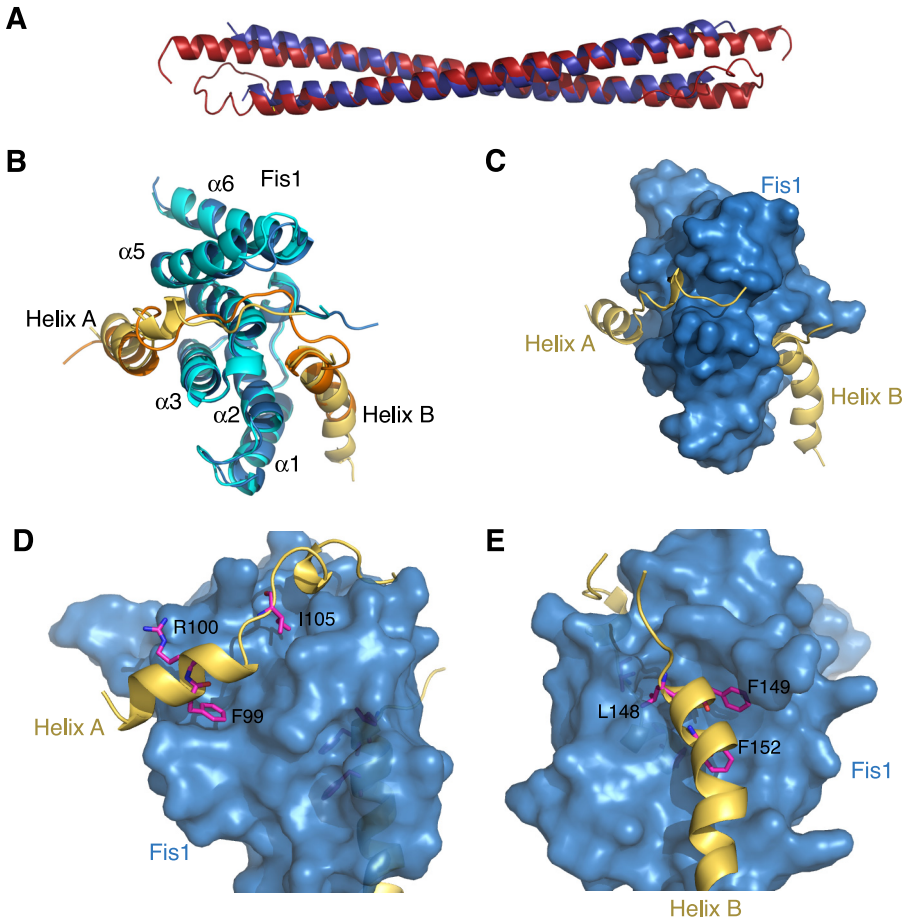

FIGURE 2. **Comparison of current Mdv1-Fis1 structure with previous structures.** *A*, superimposition of the current coiled coil (*red*) with the isolated coiled coil structure (*blue*) (26). *B*, superimposition of Mdv1-Fis1 (*yellow* and *blue*) with the previous Caf4-Fis1 structure (*orange* and *cyan*) (25). In both cases, Fis1 contains a six-helix structure that is bound by the αA-loop-αB motif of the adaptor. Several of the helices of Fis1 are labeled. *C*, binding of the Mdv1 αA-loop-αB motif (*yellow*) to the surface of Fis1 (*blue*). *D*, close-up of the Mdv1 helix αA-Fis1 interaction, highlighting three Mdv1 point mutations (stick representation) that disrupt Fis1 binding and mitochondrial fission (25). *E*, close-up of the Mdv1 helix αB-Fis1 interaction, highlighting three Mdv1 point mutations that disrupt Fis1 binding and mitochondrial fission (25).

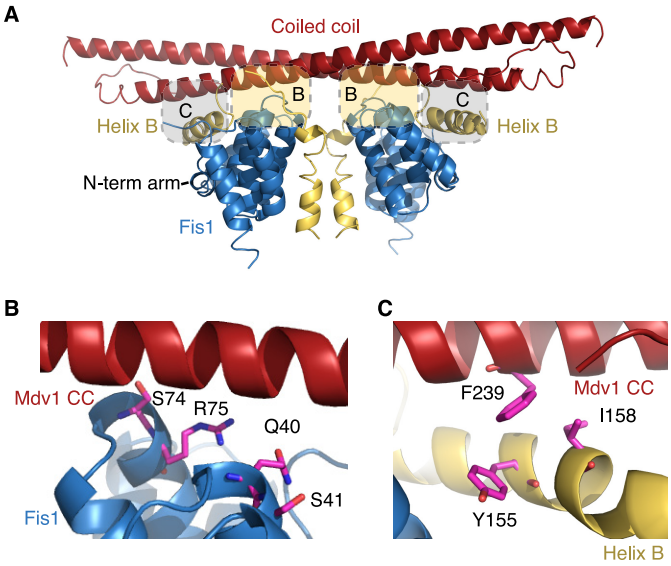

FIGURE 3. **Two binding interfaces on surface of Mdv1 coiled coil.** *A*, ribbon representation of the Mdv1-Fis1 structure, with *shaded* regions indicating interactions mediated by the long coiled coil. The *tan* shading highlights the interface shown in *B*; the *gray* shading highlights the interface shown in *C*. Because of the 2-fold symmetry of the dimer, the bottom surface of the coiled coil makes four contacts. *B*, interaction of the Mdv1 coiled-coil surface with residues on the top surface of Fis1. Residues mutated in this study are indicated (stick representation). *C*, interaction of the Mdv1 coiled-coil surface with the Mdv1 αB helix. Residues mutated in this study are indicated.

interface with Fis1, the dimeric Mdv1-Fis1 complex reveals additional unanticipated contacts between Mdv1 and Fis1 (Fig. 3*A*). The antiparallel coiled coil of Mdv1 lies on top of the two Fis1 molecules. For each Fis1 molecule, two loops (connecting helix α1 to α2 and helix α3 to α4) pack against the bottom of the coiled coil (Fig. 3, *A* and *B*). As a result, the crystal structure reveals that Mdv1 contacts three surfaces of Fis1: the concave surface, the convex surface, and the top surface.

The Mdv1 coiled coil also makes an intramolecular contact with helix αB. In the Mdv1 dimer, each αB helix crosses underneath the coiled coil in a roughly orthogonal direction (Fig. 1*C*). This helix contacts the bottom surface of the coiled coil via hydrophobic interactions (Fig. 3, *A* and *C*). As noted previously, helix αB binds to the concave surface of Fis1 and is stabilized by packing against the N-terminal arm of Fis1 (25). In the current structure, it is evident that the binding of helix αB to the Fis1 concave surface is stabilized by being sandwiched between the Fis1 N-terminal arm and the Mdv1 coiled coil (Fig. 3*A*).

Mutations in Fis1 Loops α1-α2 and α3-α4 Compromise Recruitment of Mdv1 and Reduce Mitochondrial Fission Activity—To assess the biological importance of the Mdv1 coiled coil/Fis1 interface, we constructed Fis1 mutants with two alanine substitutions adjacent to loop α1-α2 (Q40A/S41A) or loop α3-α4 (S74A/R75A) (Fig. 3*B*). Fis1 Gln-40, Ser-74, and Ser-75 are within 4 Å of polar residues on the Mdv1 coiled coil (Ser-246, Asp-253, and Ser-249, respectively). Myc-tagged Fis1 mutants were tested for physical interaction with HA-Mdv1 upon coexpression in *fis1Δmdv1Δcaf4Δ* yeast. As assayed by co-immunoprecipitation, both mutants bound Mdv1 substantially less well (Fig. 4*A*). A mutant containing substitutions with both loop regions (Q40A/S41A/S74A/R75A) also showed a large binding defect.

Consistent with the co-immunoprecipitation results, the Fis1 mutants also showed a defect in recruitment of GFP-Mdv1 to mitochondria (Fig. 4*C*). When GFP-Mdv1 was expressed alone in *fis1Δmdv1Δcaf4Δ* yeast cells, it was localized in the cytosol due to the lack of Fis1. Coexpression with wild-type Fis1 restored punctate mitochondrial localization of GFP-Mdv1 in ~80% of cells. In cells expressing the Fis1 Q40A/S41A and S74A/R75A mutants, there was a 30% reduction in the number of cells showing mitochondrial localization of Mdv1. The quadruple mutant (Q40A/S41A/S74A/R75A) showed a reduction of almost 50% (for all mutants, $p < 0.001$).

Importantly, these binding and localization profiles correlate well with mitochondrial fission activity. We quantified the ability of Fis1 variants, in combination with wild-type Mdv1, to restore tubular mitochondrial morphology in *fis1Δmdv1Δcaf4Δ* cells, which otherwise have interconnected net-like mitochondria due to a complete defect in mitochondrial fission. Whereas ~56% of yeast cells expressing wild-type Myc-Fis1 had normal tubular mitochondria, only ~17–20% of yeast cells expressing the Myc-Fis1 Q40A/S41A or S74A/R75A mutant had wild-type tubular mitochondrial morphology ($p < 0.01$) (Fig. 4*D*). Approximately 60% of these yeast cells had collapsed net-like mitochondria, the most severe fission phenotype. Similar results were found in yeast expressing the Q40A/S41A/S74A/R75A mutant. Taken together, these results indicate that the coiled coil/Fis1 interface is important for physical interaction of Mdv1 with Fis1, recruitment of Mdv1 to mitochondria, and mitochondrial fission activity.

Mutations in Mdv1 Intramolecular Interface Reduce Mitochondrial Fission Activity—In contrast to the intermolecular interface studied above, our crystal structure also identifies an intramolecular interface within Mdv1, between the coiled coil and helix αB. Based on their proximity, Tyr-155 and Ile-158 on helix αB appear to have hydrophobic interactions with Phe-239 on the coiled coil. To understand the biological function of this interface, we mutated these residues to alanine (Y155A/I158A/F239A) (Fig. 3*C*). When assessed by co-immunoprecipitation, this mutant showed slightly better binding to Fis1 (Fig. 4*B*). This mutant was properly localized to mitochondria (Fig. 4*C*) and was able to recruit Dnm1 (supplemental Fig. S1). Analysis of recombinant Mdv1-Fis1 complexes by circular dichroism did not reveal a change in secondary structure (supplemental Fig. S2). However, this mutant had a substantial defect in mitochondrial fission activity, with only 8% of cells containing normal tubular mitochondria ($p < 0.01$) (Fig. 4*D*). When these mutations were combined with the mutations in Fis1 loop α1-α2, loop α3-α4, or both, a similar loss of mitochondrial fission was observed.

DISCUSSION

Based on domain analysis, Mdv1 has a deceptively simple, modular structure, in which the NTE region binds Fis1, the coiled coil mediates dimerization, and the WD40 region binds Dnm1. However, our dimeric Mdv1-Fis1 structure reveals additional complexity that results in a surprisingly compact complex with a buried surface within the dimer of >9000 Å^2. There are four interfaces within the Mdv1-Fis1 dimer: between the Mdv1 αA-loop-αB motif and Fis1, between the helices of the antiparallel coiled coil of Mdv1, between the Mdv1 coiled coil and Fis1, and between the

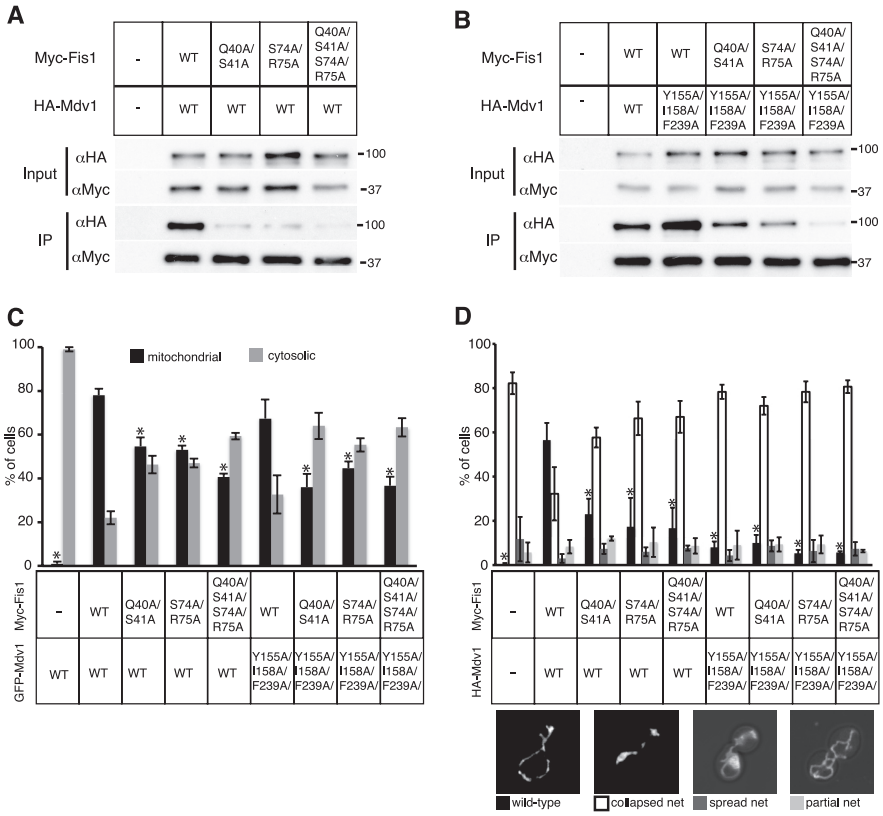

FIGURE 4. **Functional analysis of Mdv1-Fis1 interfaces.** *A*, co-immunoprecipitation of HA-Mdv1 by Myc-Fis1 variants. The mutant Fis1 constructs contain the indicated mutations. In the *lower panel*, anti-Myc immunoprecipitates were analyzed by Western blotting with anti-HA and anti-Myc antibodies. *B*, co-immunoprecipitation of HA-Mdv1 Y155A/I158A/F239A by Myc-Fis1 variants. The mutant combinations are indicated. In the *lower panel*, anti-Myc immunoprecipitates were analyzed by Western blotting with anti-HA and anti-Myc antibodies. *C*, subcellular localization of GFP-Mdv1 in yeast mutants. The localization of GFP-Mdv1 was scored as "cytosolic" when a diffuse green signal was present in the cytosol and as "mitochondrial" when green puncta were localized to mitochondria. The mutant combinations are indicated. *, $p \leq 0.001$ (unpaired *t* test) compared with wild-type Mdv1-Fis1. The Y155A/I158A/F239A mutant was not statistically different from the wild type. *D*, mitochondrial morphology in mutant yeast. Yeast cells were scored into four categories as described previously (17). Representative images of the four categories are shown. The mutant combinations are indicated. *, $p \leq 0.01$ compared with wild-type Mdv1-Fis1. In *C* and *D*, the *error bars* indicate S.D. from three independent experiments. In each experiment, 100 live yeast cells were scored.

Mdv1 coiled coil and helix αB. The latter two interfaces were unanticipated, and our mutational analysis indicated that both contribute to mitochondrial fission *in vivo*. Interestingly, these two interactions form four interfaces in the Mdv1-Fis1 dimer that cause the two Fis1 molecules to be precisely oriented in relation to the coiled coil (Fig. 3*A*). This rigidity occurs even though the loop linking the NTE to the coiled coil is unstructured.

By comparing the effects of mutations, it is clear that the interaction between the Mdv1 αA-loop-αB motif and Fis1 is more important than that between the Mdv1 coiled coil and Fis1. Nevertheless, our mutational analysis indicated that the latter contacts are functionally relevant. Our results fit well with a recent suggestion that the coiled coil of Mdv1 might play a function beyond dimerization (26). When the coiled coil of Mdv1 was swapped with a heterologous antiparallel coiled coil of similar length, the resulting molecule was only partially functional despite being able to dimerize.

In contrast, mutation of the interface between the Mdv1 coiled coil and helix αB did not disrupt binding to Fis1 or recruitment of Mdv1 or Dnm1 to mitochondria. Interestingly, though, mitochondrial fission activity was severely reduced, suggesting that this intramolecular interaction within Mdv1 plays a crucial role in mitochondrial fission via a mechanism distinct from Fis1 binding or Dnm1 recruitment. After recruiting Dnm1, Mdv1 further facilitates assembly of Dnm1 molecules into an active state (37). The interface identified in our crystal structure may have a role in this post-recruitment function.

Our results indicate that the bottom surface of the Mdv1 coiled coil plays an important scaffolding role by serving as a binding interface. Our observations also raise the question of whether the top side of the coiled coil might similarly mediate interactions with the WD40 repeat region of Mdv1. Such interactions might contribute to properly positioning Dnm1 molecules for activation. This speculation can be addressed in future structural studies.

Acknowledgments—We thank Janet Shaw for yeast strains, constructs, and helpful discussions. Some of the initial screening was done at the Molecular Observatory at California Institute of Technology, which is supported by the Gordon and Betty Moore Foundation and the Sanofi-Aventis Bioengineering Research Program. Portions of this work were carried out at the Stanford Synchrotron Radiation Lightsource, a Directorate of the SLAC National Accelerator Laboratory and an Office of Science User Facility operated for the United States Department of Energy Office of Science by Stanford University. The Stanford Synchrotron Radiation Lightsource Structural Molecular Biology Program is supported by the Department of Energy Office of Biological and Environmental Research and by National Institutes of Health National Center for Research Resources Biomedical Technology Program Grant P41RR001209 and NIGMS.

REFERENCES

1. Detmer, S. A., and Chan, D. C. (2007) Functions and dysfunctions of mitochondrial dynamics. *Nat. Rev. Mol. Cell Biol.* **8,** 870–879
2. Westermann, B. (2010) Mitochondrial fusion and fission in cell life and death. *Nat. Rev. Mol. Cell Biol.* **11,** 872–884
3. Bleazard, W., McCaffery, J. M., King, E. J., Bale, S., Mozdy, A., Tieu, Q., Nunnari, J., and Shaw, J. M. (1999) The dynamin-related GTPase Dnm1 regulates mitochondrial fission in yeast. *Nat. Cell Biol.* **1,** 298–304
4. Sesaki, H., and Jensen, R. E. (1999) Division *versus* fusion: Dnm1p and Fzo1p antagonistically regulate mitochondrial shape. *J. Cell Biol.* **147,** 699–706
5. Smirnova, E., Griparic, L., Shurland, D. L., and van der Bliek, A. M. (2001) Dynamin-related protein Drp1 is required for mitochondrial division in mammalian cells. *Mol. Biol. Cell* **12,** 2245–2256
6. Suen, D. F., Norris, K. L., and Youle, R. J. (2008) Mitochondrial dynamics and apoptosis. *Genes Dev.* **22,** 1577–1590
7. Tanaka, A., Cleland, M. M., Xu, S., Narendra, D. P., Suen, D. F., Karbowski, M., and Youle, R. J. (2010) Proteasome and p97 mediate mitophagy and degradation of mitofusins induced by Parkin. *J. Cell Biol.* **191,** 1367–1380
8. Twig, G., Elorza, A., Molina, A. J., Mohamed, H., Wikstrom, J. D., Walzer, G., Stiles, L., Haigh, S. E., Katz, S., Las, G., Alroy, J., Wu, M., Py, B. F., Yuan, J., Deeney, J. T., Corkey, B. E., and Shirihai, O. S. (2008) Fission and selective fusion govern mitochondrial segregation and elimination by autophagy. *EMBO J.* **27,** 433–446
9. Chen, H., and Chan, D. C. (2009) Mitochondrial dynamics–fusion, fission, movement, and mitophagy–in neurodegenerative diseases. *Hum. Mol. Genet.* **18,** R169–R176
10. Wakabayashi, J., Zhang, Z., Wakabayashi, N., Tamura, Y., Fukaya, M., Kensler, T. W., Iijima, M., and Sesaki, H. (2009) The dynamin-related GTPase Drp1 is required for embryonic and brain development in mice. *J. Cell Biol.* **186,** 805–816
11. Ishihara, N., Nomura, M., Jofuku, A., Kato, H., Suzuki, S. O., Masuda, K., Otera, H., Nakanishi, Y., Nonaka, I., Goto, Y., Taguchi, N., Morinaga, H., Maeda, M., Takayanagi, R., Yokota, S., and Mihara, K. (2009) Mitochondrial fission factor Drp1 is essential for embryonic development and synapse formation in mice. *Nat. Cell Biol.* **11,** 958–966
12. Waterham, H. R., Koster, J., van Roermund, C. W., Mooyer, P. A., Wanders, R. J., and Leonard, J. V. (2007) A lethal defect of mitochondrial and peroxisomal fission. *N. Engl. J. Med.* **356,** 1736–1741
13. Fekkes, P., Shepard, K. A., and Yaffe, M. P. (2000) Gag3p, an outer membrane protein required for fission of mitochondrial tubules. *J. Cell Biol.* **151,** 333–340
14. Mozdy, A. D., McCaffery, J. M., and Shaw, J. M. (2000) Dnm1p GTPase-mediated mitochondrial fission is a multistep process requiring the novel integral membrane component Fis1p. *J. Cell Biol.* **151,** 367–380
15. Tieu, Q., and Nunnari, J. (2000) Mdv1p is a WD repeat protein that interacts with the dynamin-related GTPase, Dnm1p, to trigger mitochondrial division. *J. Cell Biol.* **151,** 353–366
16. Cerveny, K. L., and Jensen, R. E. (2003) The WD repeats of Net2p interact with Dnm1p and Fis1p to regulate division of mitochondria. *Mol. Biol. Cell* **14,** 4126–4139
17. Griffin, E. E., Graumann, J., and Chan, D. C. (2005) The WD40 protein Caf4p is a component of the mitochondrial fission machinery and recruits Dnm1p to mitochondria. *J. Cell Biol.* **170,** 237–248
18. Tieu, Q., Okreglak, V., Naylor, K., and Nunnari, J. (2002) The WD repeat protein, Mdv1p, functions as a molecular adaptor by interacting with Dnm1p and Fis1p during mitochondrial fission. *J. Cell Biol.* **158,** 445–452
19. Yu, T., Fox, R. J., Burwell, L. S., and Yoon, Y. (2005) Regulation of mitochondrial fission and apoptosis by the mitochondrial outer membrane protein hFis1. *J. Cell Sci.* **118,** 4141–4151
20. Stojanovski, D., Koutsopoulos, O. S., Okamoto, K., and Ryan, M. T. (2004) Levels of human Fis1 at the mitochondrial outer membrane regulate mitochondrial morphology. *J. Cell Sci.* **117,** 1201–1210
21. Yoon, Y., Krueger, E. W., Oswald, B. J., and McNiven, M. A. (2003) The mitochondrial protein hFis1 regulates mitochondrial fission in mammalian cells through an interaction with the dynamin-like protein DLP1. *Mol. Cell. Biol.* **23,** 5409–5420
22. Koch, A., Yoon, Y., Bonekamp, N. A., McNiven, M. A., and Schrader, M. (2005) A role for Fis1 in both mitochondrial and peroxisomal fission in mammalian cells. *Mol. Biol. Cell* **16,** 5077–5086
23. Gandre-Babbe, S., and van der Bliek, A. M. (2008) The novel tail-anchored membrane protein Mff controls mitochondrial and peroxisomal fission in mammalian cells. *Mol. Biol. Cell* **19,** 2402–2412
24. Otera, H., Wang, C., Cleland, M. M., Setoguchi, K., Yokota, S., Youle, R. J., and Mihara, K. (2010) Mff is an essential factor for mitochondrial recruitment of Drp1 during mitochondrial fission in mammalian cells. *J. Cell Biol.* **191,** 1141–1158
25. Zhang, Y., and Chan, D. C. (2007) Structural basis for recruitment of mitochondrial fission complexes by Fis1. *Proc. Natl. Acad. Sci. U.S.A.* **104,** 18526–18530
26. Koirala, S., Bui, H. T., Schubert, H. L., Eckert, D. M., Hill, C. P., Kay, M. S., and Shaw, J. M. (2010) Molecular architecture of a dynamin adaptor: implications for assembly of mitochondrial fission complexes. *J. Cell Biol.* **191,** 1127–1139
27. Kabsch, W. (2010) XDS. *Acta Crystallogr. D Biol. Crystallogr.* **66,** 125–132
28. Evans, P. (2006) Scaling and assessment of data quality. *Acta Crystallogr. D Biol. Crystallogr.* **62,** 72–82
29. McCoy, A. J., Grosse-Kunstleve, R. W., Adams, P. D., Winn, M. D., Storoni, L. C., and Read, R. J. (2007) Phaser crystallographic software. *J. Appl. Crystallogr.* **40,** 658–674
30. Murshudov, G. N., Vagin, A. A., and Dodson, E. J. (1997) Refinement of macromolecular structures by the maximum-likelihood method. *Acta Crystallogr. D Biol. Crystallogr.* **53,** 240–255
31. Emsley, P., and Cowtan, K. (2004) Coot: model-building tools for molecular graphics. *Acta Crystallogr. D Biol. Crystallogr.* **60,** 2126–2132
32. Goldschmidt, L., Cooper, D. R., Derewenda, Z. S., and Eisenberg, D. (2007) Toward rational protein crystallization: a Web server for the design of crystallizable protein variants. *Protein Sci.* **16,** 1569–1576
33. Dohm, J. A., Lee, S. J., Hardwick, J. M., Hill, R. B., and Gittis, A. G. (2004) Cytosolic domain of the human mitochondrial fission protein Fis1 adopts a TPR fold. *Proteins* **54,** 153–156
34. Suzuki, M., Jeong, S. Y., Karbowski, M., Youle, R. J., and Tjandra, N. (2003) The solution structure of human mitochondrial fission protein Fis1 reveals a novel TPR-like helix bundle. *J. Mol. Biol.* **334,** 445–458
35. Suzuki, M., Neutzner, A., Tjandra, N., and Youle, R. J. (2005) Novel structure of the N terminus in yeast Fis1 correlates with a specialized function in mitochondrial fission. *J. Biol. Chem.* **280,** 21444–21452
36. Tooley, J. E., Khangulov, V., Lees, J. P., Schlessman, J. L., Bewley, M. C., Heroux, A., Bosch, J., and Hill, R. B. (2011) The 1.75 Å resolution structure of fission protein Fis1 from *Saccharomyces cerevisiae* reveals elusive interactions of the autoinhibitory domain. *Acta Crystallogr. Sect. F Struct. Biol. Cryst. Commun.* **67,** 1310–1315
37. Lackner, L. L., Horner, J. S., and Nunnari, J. (2009) Mechanistic analysis of a dynamin effector. *Science* **325,** 874–877